# A New Defected Ground Structure for Different Microstrip Circuit Applications

*Susanta Kumar PARUI, Santanu DAS*

Dept. of Electronics and Telecommunication Engg., Bengal Engg. and Science Univ., Shibpur, Howrah – 711 103, India

arkapv@yahoo.com , santanumdas@yahoo.com

**Abstract.** *In this paper, a microstrip transmission line combined with a new U-headed dumb-bell defected ground structure (DGS) is investigated. The proposed DGS of two U-shape slots connected by a thin transverse slot is placed in the ground plane of a microstrip line. A finite cutoff frequency and attenuation pole is observed and thus, the equivalent circuit of the DGS unit can be represented by a parallel LC resonant circuit in series with the transmission line. A two-cell DGS microstrip line yields a better lowpass filtering characteristics. The simulation is carried out by the MoM based IE3D software and in the experimental measurements a vector network analyzer is used. The effects of the transverse slot width and the distance between arms of the U-slot on the filter response curve are studied. This DGS is utilized for different microstrip circuit applications. The DGS is placed in the ground of a capacitive loaded microstrip line and a very low cutoff frequency is obtained. The DGS is adopted under the coupled lines of a parallel line coupler and an improvement in coupling coefficient is noticed. The proposed DGS is also incorporated in the ground plane under the feed lines and the coupled lines of a bandpass filter to improve separately the stopband and passband performances.*

## Keywords

Defected ground structure (DGS), microstrip, lowpass filter, bandpass filter, coupler.

## 1. Introduction

Wave propagation in periodic structures has been studied in applied physics for a long time [1]. Planar transmission lines with periodic structures like, photonic bandgap (PBG) have drawn a wide interest because of their extensive applicability in antenna and microwave circuits [2], [3] due to a finite pass band, rejection band and slow-wave effect. But a steep and wideband filter design by a PBG requires higher size of the circuit due to an array configuration of PBG cells. Fine-tuning of the stopband is also difficult.

A defected structure etched in the metallic ground plane of a microstrip line is one of the attractive solutions to the above problem. It obtains deep and wide stopband, sharp cutoff with its compact size to meet emerging applications. The circular headed dumb-bell shape defected ground structure (DGS) proposed by D. Ahn et al. was the first such structure investigated thoroughly [4]. Various types of DGS with different applications have appeared in the literature [5-9]. The loaded and unloaded DGS structures for CPW band-stop filter [10] have been proposed by M.F.Karim. The CPW-DGS has been applied for designing unequal Wilkinson power divider by Y-J Ko et al. [11]. Harmonics suppressions in a ring bandpass filter by using a DGS and spur line have been demonstrated by Chul-Soo Kim et al. [12].

In this paper, a new U-headed dumb-bell DGS consisting of two U-shape slots connected by a thin transverse slot is proposed. A finite cutoff frequency and attenuation pole is observed and thus, the equivalent circuit of the DGS unit can be represented by a parallel LC resonant circuit in series with the transmission line. The transverse slot in the ground plane underneath a microstrip line increases the effective capacitance and the U-shape slots attached to the transverse slot increase the effective inductance of the transmission line.

Two such DGS cells are placed under a microstrip line to obtain good lowpass filtering characteristics. This filter response can be tuned by adjusting the width of the transverse slot or the distance between the separations of the arms of the U-slot.

A coupling enhancement scheme of a parallel-line coupler is proposed by using a pair of DGS cells. High coupling coefficient is realized with a comfortable distance of separation between parallel lines, which provides more flexibility in the fabrication process.

The presence of spurious bands is a fundamental limitation of microwave filters implemented by means of distributed elements. For most of the filters, the first spurious band is relatively close to the frequency region of interest, which appears at the second harmonic of the central frequency for parallel-coupled bandpass filter [13]. In order to remove the unwanted spurious signals, a three-cell DGS is placed under both input and output feed lines of the above filter. It removes the $2^{nd}$ and $3^{rd}$ harmonics much below 30 dB and enhances stopband performances with negligible effect on the passband.

A DGS under the line resonators of the bandpass filter is proposed to enhance the passband performances. Both the electrical length and coupling effect of the resonators are modulated by the slow-wave characteristics of the DGS. The coupling effect gets enhanced for a given spacing of the resonators and thus improves the insertion loss and bandwidth. In addition to that the effective electrical length of the resonators increases which reduces the passband center frequency and thus compactness is achieved.

## 2. Characteristics of the DGS Unit

The proposed DGS unit composed of two U-shape slots (of length *p* and breath *b* and slot-arm breath *a* and length *c*) attached by a transverse slot (of length *n* and width *g*) as shown in Fig. 1(a). This DGS section can provide a cutoff frequency and attenuation pole without any periodicity like other DGS [4]. It is well known that an attenuation pole can be generated by a combination of the inductance and capacitance elements as given in Fig. 1(b). Here, the capacitance is provided by the transverse slot and the inductance by U-shape slots.

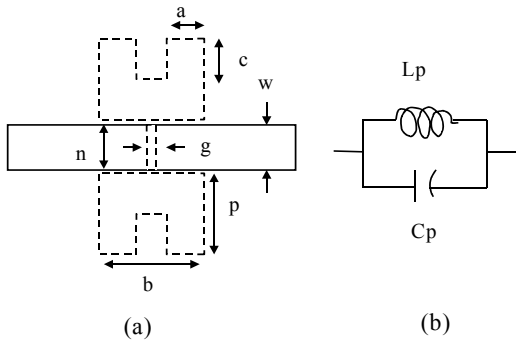


**Fig. 1.** Microstrip line with the proposed defected ground structure: (a) layout, and (b) the equivalent circuit.

The various dimensions of the structure are chosen as $b$ = 6 mm, $p$ = 4 mm, $a$ = $c$ = 2 mm, $n$ = 2 mm, and $g$ = 0.8 mm. The substrate with a dielectric constant of 3.2, loss tangent of 0.0025 and thickness of 0.79 mm is considered here. The conductor strip of the microstrip line on the top plane has a width $w$ of 1.92 mm, corresponding to 50-ohm characteristic impedance. In order to investigate the frequency characteristics of the proposed DGS section, it is simulated by MoM based IE3D EM-simulator. The simulated S-parameters of the DGS unit in Fig. 2 show the one-pole lowpass filter characteristics with an attenuation pole at 8.5 GHz and 3dB cutoff frequency at 3 GHz.

A finite cutoff frequency and attenuation pole is observed. Thus, the equivalent circuit of the DGS section can be represented by a parallel LC resonant circuit in series with the transmission line (Fig. 1(b)). To apply the proposed DGS section to a practical circuit design, it is necessary to extract the equivalent circuit parameters. The simulated result of the DGS section can be matched with the one-pole Butterworth-type lowpass filter response as given in Fig. 3. The series reactance values (Fig. 1(b)) can be easily calculated by using the prototype element value of the one-pole Butterworth response. Accordingly, the equivalent inductance $L_p$ of 4.406 nH and the capacitance $C_p$ of 0.0795 pF are extracted.

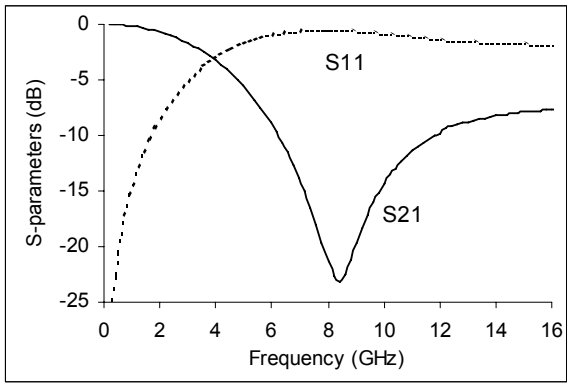


**Fig. 2.** Simulated S-parameters of DGS.

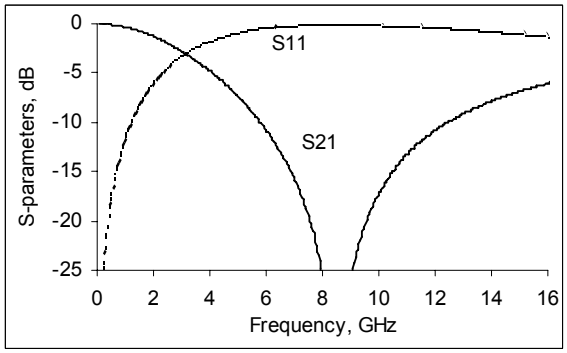


**Fig. 3.** Equivalent circuit model of DGS.

## 3. Filtering Characteristics of the Two-Cell DGS Structure

In this case, two units of the DGS sections are considered with a separation of 4 mm as given in Fig. 4. The frequency responses of the IE3D simulated S-parameters are plotted in Fig. 5. The cutoff frequency is found at 3.6 GHz. A sharpness factor of 15 dB/GHz is obtained at transition. The passband attenuation is well below 1 dB. The stopband center frequency is 6.2 GHz with a maximum attenuation of 33 dB and the 15-dB rejection bandwidth is calculated as 9.5 GHz.

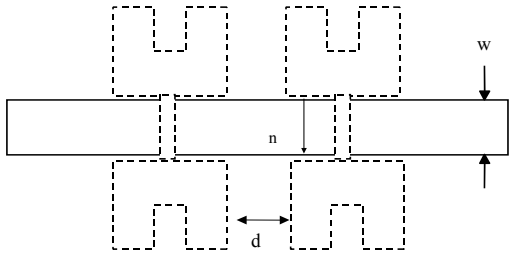


**Fig. 4.** Two-cell defected ground structure under a microstrip line.

The measurement is done by the Agilent vector network analyzer of model N5230A and the S-parameters are

plotted on the same figure (Fig.5). The measurement result shows a 3dB cutoff frequency at 3.5 GHz, a center frequency of the stopband at 6 GHz with the maximum attenuation of 42 dB and the 15-dB rejection bandwidth of 9.6 GHz. Thus, the experimental response curves match with the simulation results to a great extent. The characteristics of Fig. 5 show a three-pole lowpass filter response with low insertion loss, wide and deep stopband features.

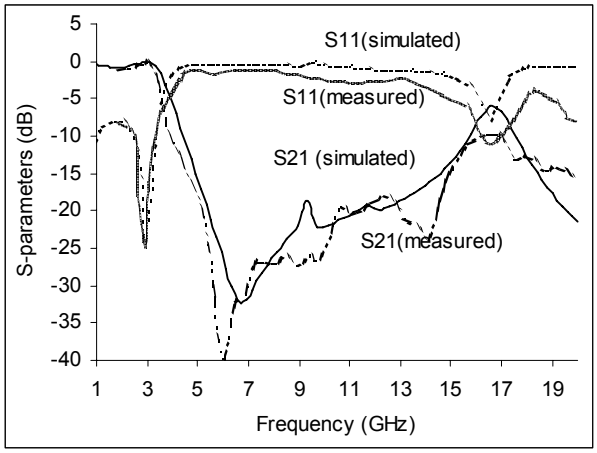


**Fig. 5.** Simulated and measured S-parameters of the Two-cell DGS.

## 3.1 Tuning by Transverse Slot Width Variation

The transverse slot width $g$ of the DGS is varied by 0.2 mm, 0.8 mm and 1.2 mm and the simulated transmission coefficients $S_{21}$ are plotted in Fig. 6. It is observed that the stopband center frequency decreases with the decrement of the transverse slot width and this is due to the increment of the lumped capacitance $C_p$.

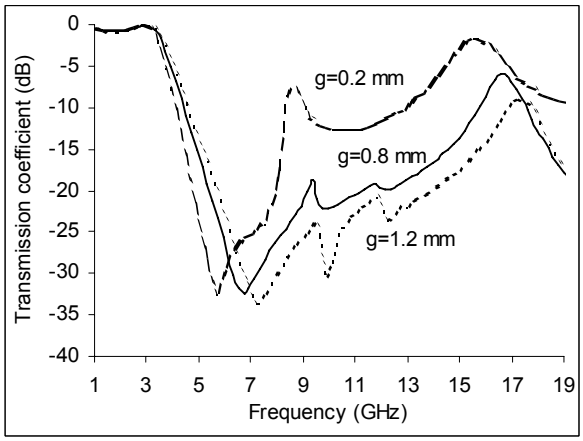


**Fig. 6.** Simulated transmission coefficient for different transverse slot width $g$ of DGS.

## 3.2 Tuning by Separation between Slot-Arms

The lumped inductance depends on the area of the aperture head of DGS [4]. But in the proposed DGS, the lumped inductance can be varied by changing the shape of U slots. If the separation $k$ between the slot-arms of the U shape aperture changes, different shapes maintaining the same etched area are built up as given in Fig. 7. The simulated transmission coefficients in Fig. 8 show that both the 3-dB cutoff frequency and stopband center frequency decrease with the increasing $k$. This is due to the increase of the lumped inductance.

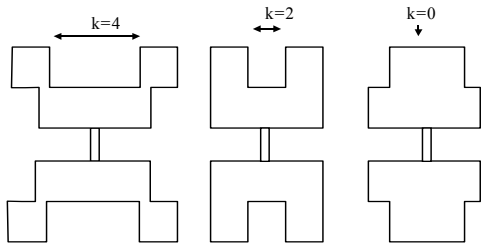


**Fig. 7.** DGS for a different value of separation $k$ between the slot-arms of U-aperture.

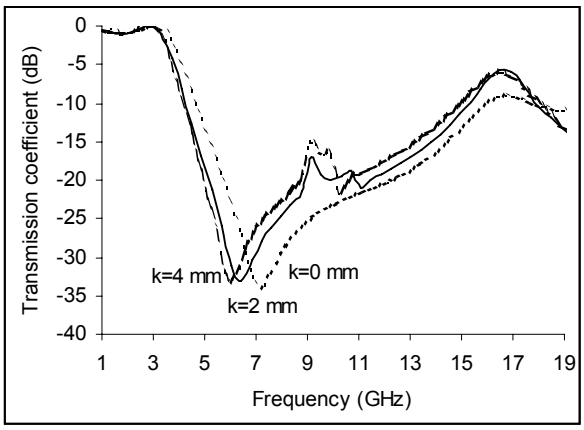


**Fig. 8.** Simulated transmission coefficient for the different distance $k$ between the slot-arms.

# 4. DGS under Capacitive Loaded Line

For a lossless microstrip line, the propagation constant, characteristic impedance and phase velocity are given as $\beta=\omega\sqrt{(LC)}$, $Z_0=\sqrt{(L/C)}$ and $v_p=1/\sqrt{(LC)}$, respectively, where $L$ and $C$ are inductance and capacitance per unit length along the line. But for a microstrip line with T-shaped loading (Fig. 9), capacitances appear resulting in a change in characteristic impedance and phase velocity expressions by $Z_{ol}=\sqrt{(L/(C+C_l))}$ and $v_{pl}=\sqrt{(1/L(C+C_l))}$ where, $C_l$ is the loaded capacitance per unit length. So a lower phase velocity, i.e., a reduced physical size can be achieved.

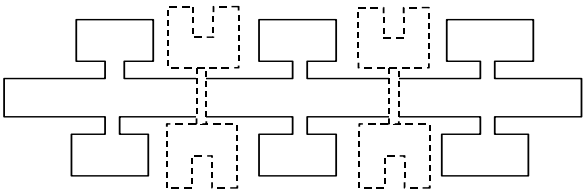

**Fig. 9.** Layout of DGS under capacitive loaded microstrip line.

Here, a double plane structure is constructed with a T-shaped capacitive loaded microstrip line on the top plane and proposed defected structures on the ground plane (Fig. 9). In order to make an investigation as well as maintain symmetry, three numbers of T structures and two DGS cells are considered. The T structure consists of a patch (4.8 mm x 2.4 mm) with a stem (1.2 mm x 0.8 mm) and is placed at a periodic distance of 9.6 mm. The DGS has the dimensions of $b$ = 4 mm, $p$ = 4 mm, $a$ = 1.4 mm, $c$ = 2 mm, $g$ = 0.4 mm and $n$ = 2 mm.

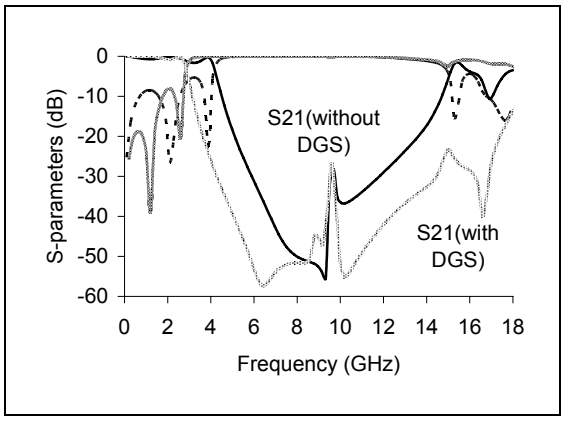


**Fig. 10.** Simulated S-parameters of capacitance loaded microstrip line with and without DGS.

The 20-dB rejection bandwidth is 8.5 GHz and the cutoff frequency is 3.9 GHz for the capacitive loaded microstrip line (Fig.10), whereas these parameters are 12 GHz, 2.8 GHz, respectively for the same line with the DGS. Thus, a wide stopband is clearly observed from the simulated plots of Fig. 10 for the capacitive loaded microstrip line with the DGS. So, the filtering performance of the capacitive loaded microstrip line is dramatically improved by the introduction of U-headed dumbbell DGS. Moreover, ultra low cutoff frequency is achieved with almost the same overall dimension of the filter. It then may be put in the category of very compact filter.

## 5. Coupling Enhancement of Parallel-Line Coupler by DGS

A coupling enhancement scheme of a parallel-line coupler by using a pair of proposed DGS cells is proposed in Fig. 11. The coupling coefficient is defined by: $S_{41} = \left| \mathrm{Sin}\,(\pi \Delta n_{\mathrm{eff}} Lf/c) \right|$ where $\Delta n_{\mathrm{eff}} = \sqrt{\varepsilon_{\mathrm{effe}}} - \sqrt{\varepsilon_{\mathrm{effo}}}$. $\Delta n_{\mathrm{eff}}$ is the effective dielectric constant; $\varepsilon_{\mathrm{effe}}$ is the dielectric constant for even mode; $\varepsilon_{\mathrm{effo}}$ is the dielectric constant for odd mode. So the efficiency of the coupler can be designed if effective dielectric constant is controlled.

A wave travels longer path in even modes, signals slow down and the phase velocity decreases. Therefore, the effective dielectric constant increases. In odd mode E-field pattern is asymmetric i.e., E-field is continuous even in presence of a DGS. So the signal path in odd mode is exactly the same as without a DGS. Hence waves do not experience any slowwave effect and thus the dielectric constant for odd mode remains unchanged. Therefore, the effective dielectric constant $\Delta n_{\mathrm{eff}}$ increases with the inclusion of a DGS and thus, the coupling coefficient enhances.

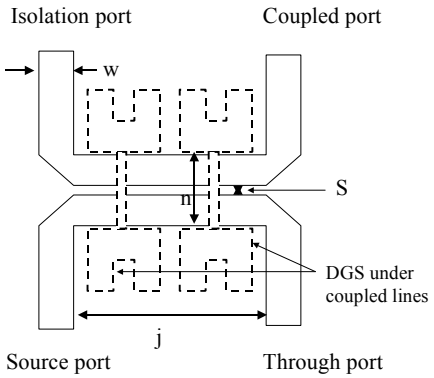


**Fig. 11.** Layout of parallel-line coupler integrated with DGS.

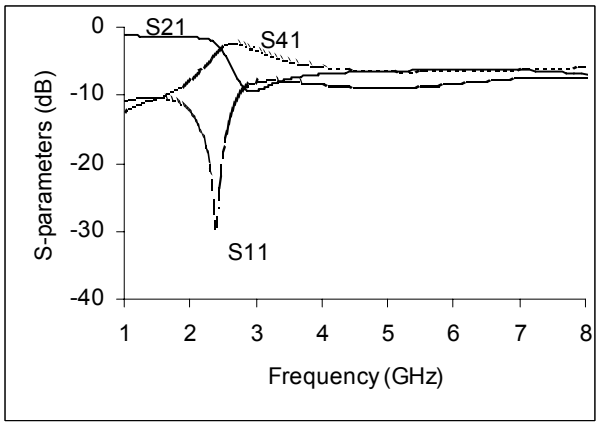


**Fig. 12.** Simulated S-parameters of the coupler with DGS.

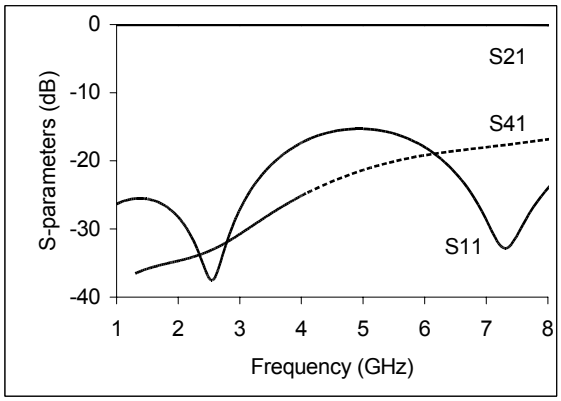


**Fig. 13.** Simulated S-parameters of the parallel line coupler.

For our DGS coupler, the different dimensions are $w$ = 1.92 mm, $j$ = 18 mm, $s$ = 0.5 mm, $b$ = 6 mm, $p$ = 4 mm, $a$ = $c$ = 2 mm, $g$ =1mm, $n$ = 5 mm and $d$ = 4 mm. The layout is shown in Fig. 11. The simulated scattering parameters of the DGS coupler are plotted in Fig. 12. The transmission coefficient $S_{21}$ attenuates with a deep of 10 dB at the frequency of 2.8 GHz and the coupling coefficient $S_{41}$ rises to –3 dB at nearly the same frequency, whereas, $S_{21}$ and $S_{41}$ show these values at –0.1 dB and -23 dB respectively for the coupler without the DGS (see Fig. 13).

So it can be said that the inclusion of the DGS prevents the direct transfer of power from the source port to the through port in the vicinity of 2.8 GHz and most of the power transmits to the coupled port. A bandstop is observed in transmission characteristic and thus, the energy stored in the DGS is transferred to the non-excited line causing coupling. A coupling of 3-dB is achieved by maintaining a comfortable distance of separation between the two parallel lines, which provides more flexibility in the fabrication process. Such a coupler can be designed at the desired frequency by choosing the appropriate stopband of DGS.

# 6. Performance Enhancement of a Bandpass Filter by DGS

Here a three-pole microstrip parallel-coupled bandpass filter (BPF) using half-wavelength line resonators is presented the layout of which is in Fig. 14(a) [13]. The adjacent resonators are completely parallel to each other and therefore give relatively larger coupling for a given spacing between the resonators and reduce the overall size of the filter. The length of line resonators is 26 mm for passband center frequency at 3.5 GHz [13]. The width of resonators is taken as 2 mm. The width of the feed line is 1.92 mm towards ports and 0.5 mm towards resonators. The gap is 0.4 mm between resonators and 0.2 mm between the feed line and the resonator.

From the simulated transmission coefficient (Fig. 14(b)) it is found that the passband center frequency is 3.5 GHz with 3dB bandwidth of 410 MHz (12%). Higher harmonics are observed at around 6.8 GHz and 10.4 GHz.

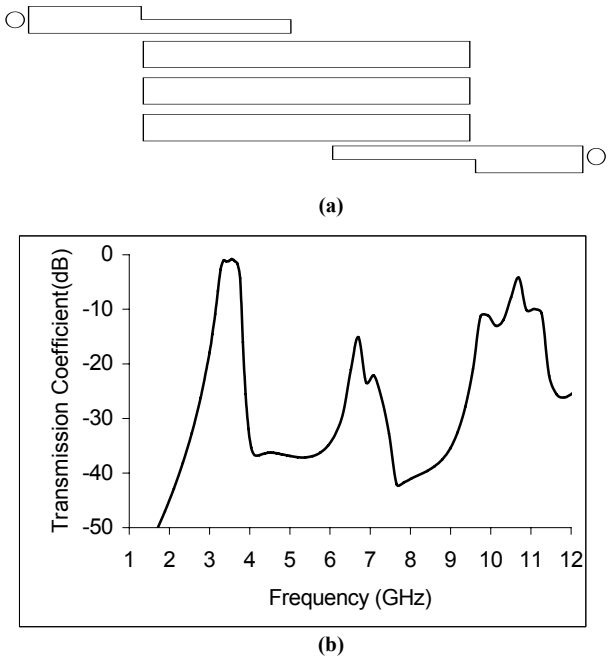


**Fig. 14.** Parallel-coupled bandpass filter: (a) layout; (b) Simulated transmission coefficient.

## 6.1 Stopband Tuning

A layout of the above BPF incorporating 3-cell DGSs in the ground plane under the feed lines is given in Fig. 15(a). Here, the DGS etched under both input and output feed lines behaves like a lowpass filter and allows the fundamental frequency to pass rejecting harmonics. The DGS line should have substantially high sharpness factor and wide stopband characteristics. The higher sharpness of the stopband of the DGS offers less passband insertion loss and also, high attenuation to the 1st harmonic of BPF. A wide stopband of DGS rejects more numbers of harmonics. The cutoff frequency of DGS line is chosen at the edge of the passband (here 4 GHz) of BPF to minimize the insertion loss. A high attenuation (at least 40 dB) and sharpness (about 20dB/GHz) of DGS line is required for removal of the first harmonic effectively. The two-cell DGS line offers a sharpness factor of 15 dB/GHz as mentioned earlier. Due to this fact it is not possible to completely remove the 1st harmonic of the BPF maintaining low insertion loss in the passband (by using a two-cell DGS).

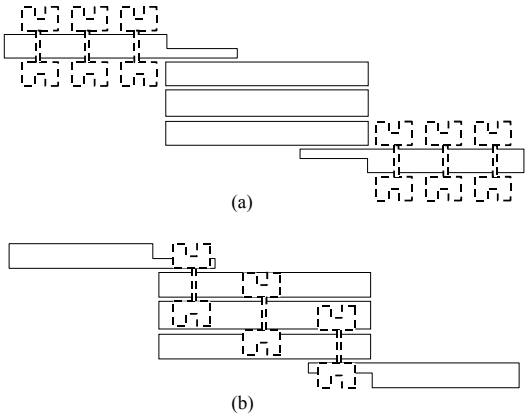


**Fig. 15.** Layout of BPF: (a) DGS under feed lines and (b) DGS under coupled lines.

As the number of cells in a DGS line increases, the sharpness factor and bandwidth increases. But the total dimension of the DGS line also increases. Hence an optimum 3-cell DGS line is chosen. The simulated S-parameters of a 3-cell DGS line are in Fig. 16. The dimensions of this DGS cells are $b$= 4.5 mm, $p$ =4 mm, $a$ =1.5 mm, $c$= 2 mm, $g$= 0.4 mm, $n$=2 mm, and $d$= 1 mm. The spacing between two cells is taken 1.1 mm. The 3-dB cutoff frequency, stopband center frequency and maximum stopband attenuation are 4.8 GHz, 6 GHz and 34 dB respectively. A sharpness factor of 30 dB/GHz is also achieved at transition knee, which is sufficient to fulfill the design criteria. It also offers 15dB deep attenuation from 5 to 12 GHz, which can easily remove higher harmonics.

The simulated and measured transmission coefficients of the BPF with DGS feed line are plotted in Fig. 17. It is observed that the attenuation of the 2nd and 3rd harmonics is well below 30 dB and the stopband extends up to 12 GHz. The passband center frequency remains at 3.45 GHz. Therefore, a wide stopband without any appreciable change in the passband characteristics can be achieved.

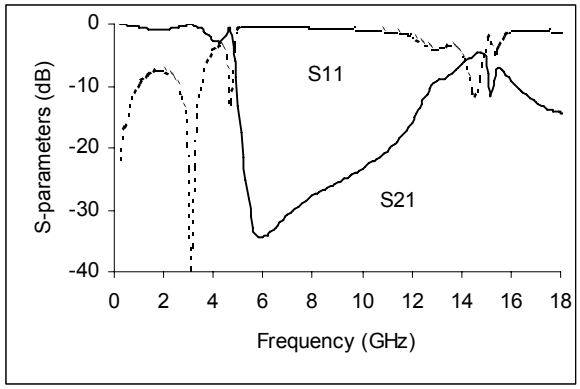


**Fig. 16.** Simulated S-parameter of 3-cell DGS line.

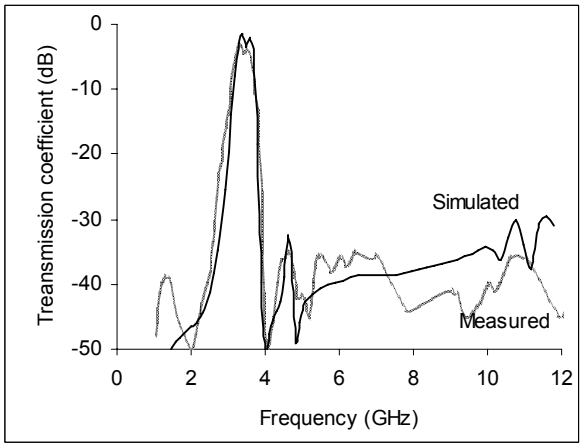


**Fig. 17.** Transmission coefficient of BPF with DGS under feed lines.

## 6.2 Passband Tuning

The slow-wave factor of a DGS increases towards the edge of stopband. So if the passband of a BPF is designed near the edge of the stopband of DGS, the maximum effect of slowwave characteristics can be availed. Due to slow-wave, the effective electrical length of resonators increases. Therefore, the cutoff frequency decreases and thus provides compactness in design. A DGS etched in the metallic ground plane under the coupled lines of a parallel coupled BPF enhances the coupling between the lines due to slow-wave effects and therefore, yields higher bandwidth of the filter.

In this work, three DGS cells are etched under line resonators as shown in Fig. 15(b). The dimensions of the DGS cells are chosen such that the passband of the band-pass filter is kept close to the stopband edge frequency of the DGS and the maximum slow-wave factor is obtained. Accordingly, the dimensions of the DGS cells are $b$ = 4.5 mm, $p$ = 4 mm, $a$ = $c$ = 1.5 mm, $g$ =0.4 mm and $n$ = 2 mm. The simulated and measured transmission coefficients are drawn against frequency in Fig. 18. A 3-dB bandwidth of 1.2 GHz is obtained around the center frequency of 3.1 GHz from the measurement result, whereas it is 1.5 GHz around the center frequency of 3 GHz in the simulated result. Thus a fractional bandwidth around 40% is achieved, which is 3.5 times more than the BPF without a DGS as shown earlier in Fig. 14(b). It yields excellent selectivity of 50 dB/GHz on both edges of the passband. But the response shows poor stop-band performance due to the harmonics developed around 5.4 GHz. By varying the dimensions of the DGS cells, the slow-wave factor can be modified and as a result, the bandwidth of the filter can be tuned. So, this method may suitably be utilized for controlling the bandwidth of this BPF. This is of particular importance when there are limitations in controlling the spacing between the coupled lines of this type of filter to get variation in bandwidth.

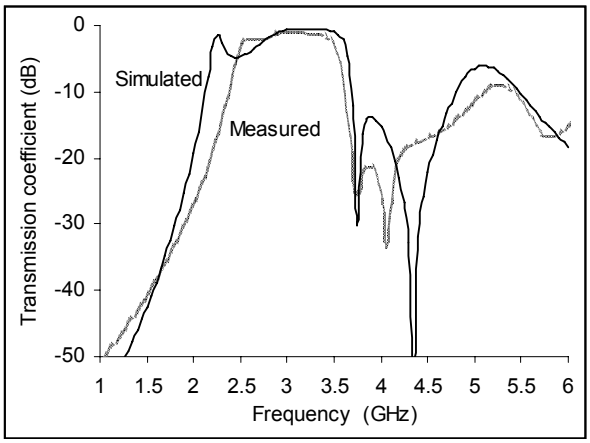


**Fig. 18.** Simulated and measured transmission coefficients of BPF with DGS cells under coupled lines.

## 6.3 The Design of High Performance Filter

It is seen that the DGS etched in the metallic ground plane under coupled lines yields higher bandwidth and higher selectivity at the cost of poor stopband performances. In order to remove the unwanted harmonic frequency components appearing in such case, the DGSs can also be used in the ground plane under the input and output feed lines (Fig. 19) as describe earlier.

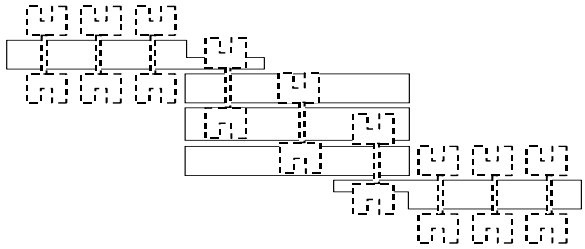

**Fig. 19.** Layout of BPF using DGS under both feed and coupled lines.

Therefore, high performance of the filter can be achieved with an improved passband as well as stopband by incorporating DGSs under both feed lines and coupled lines simultaneously as shown in Fig. 19. The performance enhancement for both the passband and stopband is clearly observed in the simulated transmission coefficient plotted in Fig. 20. Besides, the compactness of the filter is achieved due to lowering of the passband center frequency.

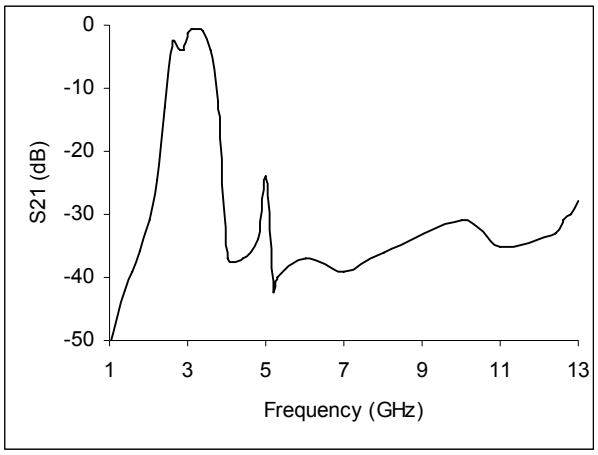


**Fig. 20.** Simulated S-parameter of BPF using DGS under both feed and coupled lines.

# 7. Conclusion

A new U-headed dumb-bell defected ground structure, which combines two U-shaped slots by a thin transverse rectangular slot, is proposed. A two-cell of the above DGS under microstrip line shows lowpass as well as bandstop characteristics and its stopband can be tuned by varying the distance between the slot-arms of the U-shape aperture and the transverse slot width. By superposition of a microstrip line with T-shaped loading and proposed defected structures on ground plane, a deep and wide stopband characteristic is achieved at ultra low cutoff frequency. A coupling enhancement scheme of a parallel-line coupler is proposed by using the DGS. A high coupling coefficient with comfortable distance of separation between lines is achieved. A new technique to enhance the stopband as well as passband performances of a parallel-coupled bandpass filter by incorporating the DGSs under feed lines and coupled lines is proposed. This scheme might be utilized in all kinds of filter design in general.

# References

[1] YABLONOVITCH, E. Photonic crystals. *J. Modern Opt.,* 1994, vol. 41, no. 2, p. 173 - 194.

[2] RADISIC, V., QIAN, Y., COCCIOLI, R., ITOH, T. Novel 2-D photonics bandgap structure for microstrip lines. *IEEE Microwave Guided Wave Lett.,* 1998, vol. 8, no. 2, p. 69 - 71.

[3] PARUI, S. K., DAS, S. A simple electromagnetic bandgap structure for microstrip line. In *Proceedings of the IEEE India Annual Conference.* 2004, p. 547 - 548.

[4] AHN, D., PARK, J. S., KIM, C. S., KIM, J., QIAN, Y., ITOH, T. A design of the low-pass filter using the novel microstrip defected ground structure. *IEEE Trans. Microwave Theory Tech*., 2001, vol. 49, no. 1, p. 86 - 93.

[5] KIM, C. S., PARK, J. S., AHN, D., LIM, J. B. A novel 1-D periodic defected ground structure for planar circuits. *IEEE Microwave Guided Wave Lett.,* 2000, vol. 10, no. 4, p. 131 - 133.

[6] LIM, J. S., KIM, C. S., LEE, Y. T., AHN, D., NAM, S. Design of lowpass filters using defected ground structure and compensated microstrip line. *IEE Electronics Lett.,* 2002, vol. 38, no. 22, p. 1357 to 1358.

[7] LIU, H., LI, Z. Enhanced Hi-Lo microstrip lowpass filter using nonuniform defected ground structure (DGS) slots. *J. of Active and Passive Electronic Devices,* 2005, vol. 1, p. 35-40.

[8] ABDEL-RAHMAN, A. B., VERMA, A. K., BOUTEJDAR, A., OMAR, A. S. Control of bandstop response of Hi-Lo microstrip low-pass filter using slot in ground plane. *IEEE Trans. Microwave Theory Tech.*, 2004, vol. 52, no. 3, p. 1008 - 1013.

[9] LIU, H., LI, Z., SUN, X., Compact defected ground structure in microstrip technology. *IEE Electronics Lett*., 2005, vol. 41, no. 3, p. 132 - 134.

[10] KARIM, M. F., LIU, A. Q., ALPHONES, A., J. ZHANG, X., YU, A. B., CPW Band-stop filter using unloaded and loaded EBG structures. *IEE Proc. Microwave Antenna Propagation*, 2005, vol. 52, no. 6, p. 434 - 440.

[11] KO, Y-J., PARK, J-Y., BU, J-U. Fully integrated unequal Wilkinson power divider with EBG CPW. *IEEE Microwave and Wireless Components Lett*., 2003, vol.,13, no. 7, p.,276 - 278.

[12] KIM, C-S., KIM, D-H., SONG, I-S., LEONG, K. H., ITOH, T., AHN, D. A design of a ring bandpass filters with wide rejection band using DGS and spur-line coupling structures. In *Proceedings of IEEE Conference*. 2005, p. 2183-2186.

[13] HONG, JIA-SHEN., G., LANCASTER, M. J. *Microstrip Filters for RF/Microwave Applications.* John Willey & Sons, Inc., 2001.

# About Authors…

**Susanta Kumar PARUI** (1965) received the B.Sc degree in Physics, and the B.Tech. degree in Radiophysics and Electronics from the University of Calcutta in 1987 and 1990, respectively. He has done the Master degree in Microwave Communication Engineering from the Bengal Engineering College, India in 1993. From 1993 to 2000, he worked as Instrument Engineer. Since 2000, he is associated with the Department of Electronics and Telecommunication Engineering, Bengal Engineering and Science University, India and presently holds the post of Senior Lecturer. His current research interests include the planar circuits, filters, antenna elements and electromagnetic bandgap structures.

**Santanu DAS** (1968) received the B.E. degree in Electronic and Telecom. Engineering from the Bengal Engineering College in 1989, and the M.E degree in Microwave Engineering from the Jadavpur University, Calcutta in 1992. He obtained the Ph.D (Engineering) degree in the year 1998 from the Jadavpur University. As Lecturer in Electronics and Telecommunication Engineering, he joined the department of the Bengal Engineering and Science University in 1998 and presently holds the post of Assistant Professor. His current research interests include the microstrip circuits, antenna elements and arrays, FSS and defected ground structures. He is a life member of the Institution of Engineers, India.